



Original Article

ISSN : 2277-3657
CODEN(USA) : IJPRPM

The Use of Microcomputed Tomography to Study the Anatomical Features of the Body

Sergey Viktorovich Pushkin^{1*}, Olga Igorevna Chistohina², Amina Islyamovna Turalieva²,
Svetlana Ruslanovna Subaeva², Diana Armenovna Karapetyan², Alexandra Alexandrovna
Romanova², Yulia Alexandrovna Zhatko²

¹Department of Biology, Medical and Biological Faculty of North Caucasus Federal University, Stavropol, Russia.

²Department of Therapy, Faculty of Medicine of Astrakhan State Medical University, Astrakhan, Russia.

*Email: sergey-pushkin-st@yandex.ru

ABSTRACT

The article describes the results of a microcomputed tomography study of the anatomy of *Nicrophorus satanas*. The purpose of the study was to describe the anatomical and morphological structure of the species using microtomographic microscopy as well as to prepare and develop methods that could be used in subsequent experiments of this kind. Due to the large body size characteristic of this species, it has developed pronounced body muscles. Interrelated with this was an especially strong development of the respiratory system with large tracheas permeating the entire body. The number of neurons in *N. satanas* is not large, but despite this, the relative volume of the central nervous system is much higher. This suggests the conclusion that an increase in the volume of the nervous system becomes possible when the beetles become big enough. At the same time, we observed fundamental differences in the structure of the central nervous system, which are associated with complex behaviors. The perception of odors and analysis thereof (smell of a carcass, a pheromone, an attractant), as well as the perception of sound signals (designed to attract the opposite sex or to warn of imminent danger), have contributed to the development of the central nervous system. The data obtained will help us to further monitor the development of the central nervous system in the *Nicrophorus* genus in the context of the evolution it went through when transitioning to the necrobiontic lifestyle.

Key words: *Nicrophorus satanas*, Burying beetles, μ CT microscopy, Anatomy

INTRODUCTION

Methods of 3D visualization of biological samples are experiencing unprecedented development, and tools such as X-ray microcomputer tomography are becoming more and more accessible to biologists [1]. Computed X-ray microtomography (μ CT) makes it possible to study the internal structure of the object under study without threatening its integrity [2]. In recent years, this method has been increasingly used to study the structure of insects [3]. However, in Coleoptera, soft tissues are practically indistinguishable from each other in density, which makes this method unsuitable in this case [4]. We were able to eliminate this shortcoming by applying contrast treatment to our research object and switching our CT scanner to low accelerating voltage and low current mode. The use of computer microtomography allows the researcher to obtain a continuous series of cross-sections (each available in three types) of the sample under study [5].

Dense materials, such as chitin, usually do not require any special preparation. Soft tissue samples, the visualization of which may be difficult due to the low absorption of X-rays, are examined using contrast agents

(we used iodine) [6]. A live image of whole coleoptera invertebrates can be performed using X-ray microcomputer tomography with a spatial resolution of 10-100 μm [3, 7].

The purpose of this scientific work is to show the possibility of using the methods of MKCT in the study of the anatomy of gravediggers. In this case, the object under study can subsequently be used for other anatomical studies: direct autopsy or dissection of the brain.

Silphidae is a small family of beetles found in the Palearctic region and is divided into two subfamilies: Nicrophorinae and Silphinae [8]. The first subfamily has a more homogeneous taxonomic composition and a greater biological similarity than the second [9, 10]. Burying beetles bury the carcasses of small vertebrates, which they later feed on and grow their larvae. Interesting exceptions are *Nicrophorus pustulatus*, a species that feeds on the eggs of some snakes, and *Nicrophorus morio*, which preys on the larvae of other necrobionts [8, 9]. Nicrophorinae is characterized by a complex reproductive biology described by Fabre, which includes the care of both parents for the young [10]. Chemical signals used by Nicrophorinae beetles have also been studied relatively closely [11]. It has been shown that *Nicrophorus* beetles in the imago stage can sense volatile substances emanating from the carcass at a distance of several kilometers [10]. It was found that some beetle species use cuticular hydrocarbons to identify individuals of different species and ages at close range [12].

Figure 1a shows a general view of the beetle body structure [13]. The length of the beetle is 2.0–3.8 cm. As can be seen in **Figure 2b**, the length of this individual is 3.75 cm. It has broad bicolored antennae that end in dark yellow or brown apical segments. The pronotum is broad and thyroid. Elytra are black or chestnut with brown arches. The epipleura has the same color as the elytra. There are only individual hairs on the epipleural ribs on the shoulders of the elytra. The posterior tibia has strongly pronounced hump-like protrusions that extend outward. The eyes and lower jaws are large and have a pronounced seam.

Nicrophorus satanas beetles are necrophages and necrobionts: they feed on carrion both at the imago stage and larvae [14]. Beetles bury carcasses of small animals in the soil and provide a high level of care for their offspring, larvae, preparing a nutrient-rich substrate for them. An interesting feature of this species is that, although the larvae can feed on their own, the parents still prefer to feed them a kind of nutritious "broth", which they get by dissolving the carcass tissues with digestive enzymes [8]. This allows the larvae to develop faster (within 20-25 days).

MATERIALS AND METHODS

Beetles were collected using hunting cylinders with bait-ground beef in the vicinity of Neftekumsk (Stavropol Territory, Russia). Males and females were kept in pairs, in plastic cages measuring 20:25:30 cm. The soil was used as a mixture: of river sand, chernozem, and forest humus, in proportions: 1:1:2. The corpses of *Mus musculus* mice were placed in beetles' cages as a food source [15]. The behavior of beetles was monitored in the morning and evening hours, which corresponds to the nature of their activity [8].

When *N. satanas* beetles find a carcass, they begin to struggle for dominance over the resource. Heavier and larger-bodied beetles tend to win. The losing females sometimes lay eggs next to the carcass, and some of their offspring can get into and develop in the nest of the winning beetles [16]. In larger species, males fight males, and females fight females. The winners, male and female, work together to bury the carcass by digging under it. If the substrate is too hard, the couple can move the carcass to a more suitable soil by climbing under it and moving it with their feet [17]. If a male finds a carcass and there are no females nearby, he climbs onto something tall next to the carcass, raises the tip of his abdomen high into the air, and emits a pheromone to attract a female [18]. Females can store sperm for later use, and sometimes they can find and bury corpses alone. The fur or feathers are removed from the carcass and a brood chamber is built in which the carcass and developing larvae will be housed [18]. The carcass is treated with oral and anal secretions, which help to preserve the product from microbial decomposition. Then the female lays eggs depending on the mass of the carcass (typically 10-30 eggs). Since body size is crucial to winning carcass contests, this species has developed a behavior known as filial cannibalism – parents kill and consume "extra" larvae, which would otherwise reduce the average body size of the resulting offspring [11, 19]. Parents feed their larvae to the last stage of their development, regurgitating a kind of "broth" consisting of a partially digested mass of carrion.

Microtomography method

There are two methods of μCT microscopy:

1. Without using a filter (this method allows you to identify all objects, even barely noticeable, but can lead to the appearance of artifacts in the image).
2. Using only one filter (the thinnest available), which can eliminate artifacts by reducing the level of detail (poor contrast).

For this study, the first method was chosen.

The research work within the framework of the project entitled “Microtomographic study of *Nicrophorus satanas*” was carried out based on the interdepartmental scientific and educational laboratory of experimental Immunomorphology, Immunopathology, and Immune Biotechnology at the Institute of Living Systems of the North Caucasus Federal University using the Microscan 1176 microtomographic scanner (Bruker, Belgium).

The object of the study was samples of *Nicrophorus satanas*, previously fixed in 70% ethanol.

The samples were X-rayed to reduce turbidity [20] using the following methods:

1. sample fixation in ethanol;
2. soaking the sample in 1% alcohol solution J2 for 72 hours;
3. washing the sample with 96% ethanol (5 minutes).

NRecon software (1.7.4.2, Bruker-microCT, Belgium) was used to reconstruct the scanned images. The Data Viewer software (1.5.6.2, Bruker-microCT, Belgium) was used to set the spatial orientation parameters (x, y, z) and select individual reconstruction areas. CT-Analyzer software (1.18.4.0, Bruker-microCT, Belgium) was used for data visualization and analysis. CTVox software (3.3.0r1403, Bruker-microCT, Belgium) was used to provide 3D visualization of the results obtained depending on the X-ray density.

Articles describing microscopy methods using a microtomographic scanner were analyzed [21, 22].

RESULTS AND DISCUSSION

The data on the anatomy of the species are presented in **Figures 1-6**. The article presents original research on microtomography Skyscan 1176 Bruker, as well as the study of the brain using the Nissl technique [23].

The general view of the internal structure (**Figure 2a**) shows that the intestinal tract occupies the medial region of the body cavity, the muscles occupy most of the thorax, the entire inter-organ space is filled with fat body cells, the only large unoccupied cavity is the intestinal tract (**Figure 4a**), the nervous system is well developed and concentrated in the head and thorax (**Figure 2a**), the reproductive system occupies a significant part of the apical segments of the abdomen (**Figure 2b**), the heart is well visualized (**Figure 4b**), and the diaphragms are well developed (**Figure 3**), nerve cord (**Figure 6a**), male genital system (**Figure 6b**).

The integuments of the species, like in most Coleoptera [19], are composed of the cuticle, the hypodermis, and the basal membrane. The cuticle is about 25 microns thick. It consists of the epicuticle, which is about 200nm thick, and the poorly delimited exo- and endocuticle. The latter two have lamellar structures everywhere except for the intersegment areas, where they are homogeneous. The hypodermis, which is composed of flattened cells, is 3–5 microns thick (**Figure 4a**).

The main elements of the endoskeleton of Coleoptera adults [24] are the tentorium and the metendosternite. The tentorium, like in other Silphidae beetles, consists of a base, a corporotentorium, as well as the anterior, dorsal, and posterior arms. Similar structures have also been observed in small Ptiliidae. The structure of the metendosternite, regarded as a conservative feature as far as the higher classification of beetles is concerned [24], is composed of two branches that are widely spaced apart (**Figure 2**).

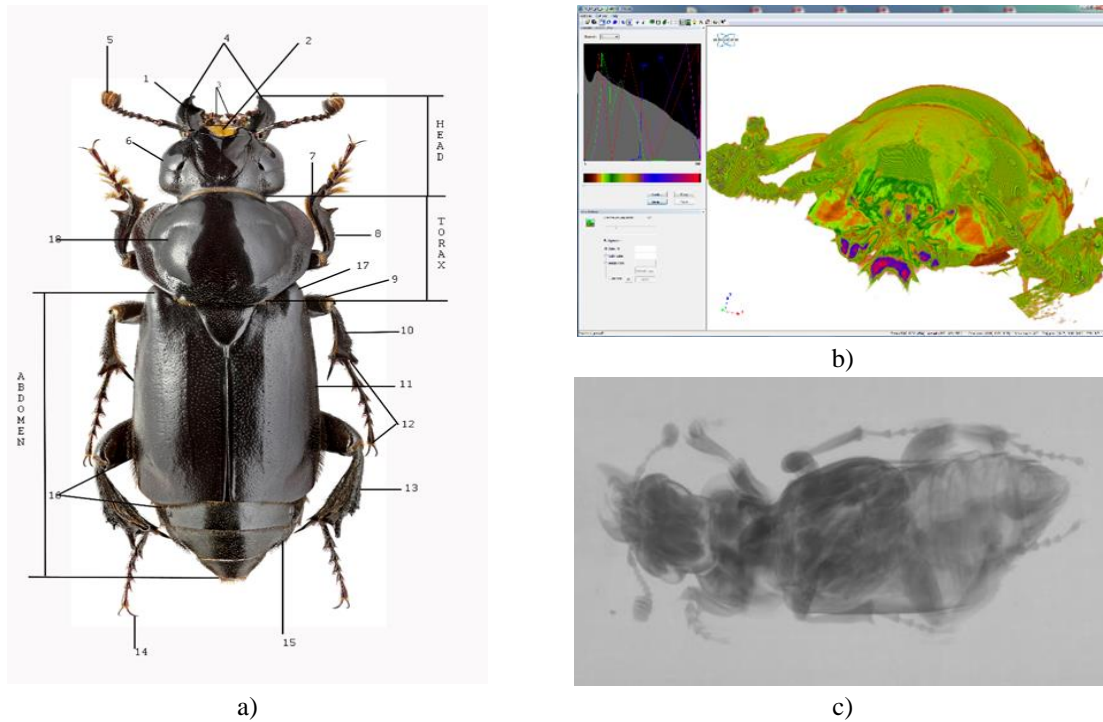


Figure 1. a) Morphological description: 1- mandibular channel; 2- clupeus; 3-maxille; 4- mandible; 5- clavate antenna; 6- oculus; 7- protarsus; 8- tibial; 9- femur; 10- midtarsus; 11- elytra; 12- tarsomeres; 13- hindtarsus; 14- claw; 15- abdomen; 16- chaetae; 17- humeri; 18- pronotum (torax); Head. Thorax. Abdomen; b) Image processing template: (screenshot); c) X-ray to scan: photo before scanning.

By and large, the structure of the digestive system of the species matches the overall pattern shared by insects [24]. The alimentary canal is subdivided into the fore-, mid-, and hindgut. The fore- and hindgut are of ectodermal origin and have a cuticular lining (Figures 2 and 3). The midgut is of endodermal origin and does not have such a lining, which makes it poorly visualizable. The intestinal canal is slightly longer than the body and forms a loop in the posterior thorax (Figure 2b). The only type of digestive glands detected were the labial salivary glands (Figure 2).

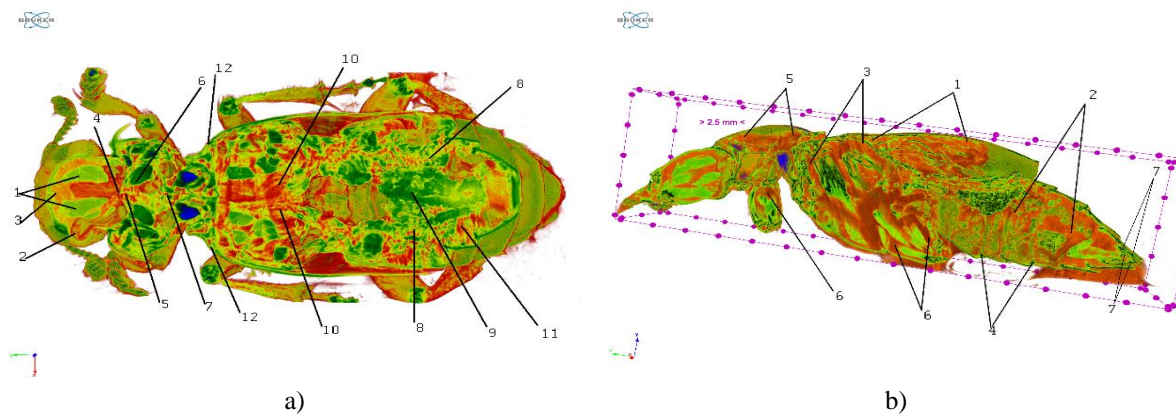


Figure 2. a) Top view of the location of the internal organs: 1- brain; 2- compound eye; 3-neurosecretory cells of brain; 4- corpus cardiacum; 5- hypopharynx; 6-prothoracic gland; 7- crop; 8- malpighian tubules; 9- hindgut; 10- ventral diaphragm; 11- septa diving appendages; 12- trachea; b) Longitudinal section of the body: 1- Alary muscles; 2- tergal longitudinal muscles; 3- sternal longitudinal muscles; 4- spiracles; 5- chest muscles; 6- thigh muscles; 7- reproductive system.

The foregut appears to be divided into the pharynx/esophagus system, the goiter (Figure 2a), and the muscular stomach (Figure 3). The pharynx is quite large in diameter and has strong muscles (Figure 2), which may reflect the fact that the animal feeds on soft food [19]. The esophagus is straight, its diameter is 160 microns, and it has many layers of ring muscles and a layer of longitudinal muscles (Figure 2b) [24].

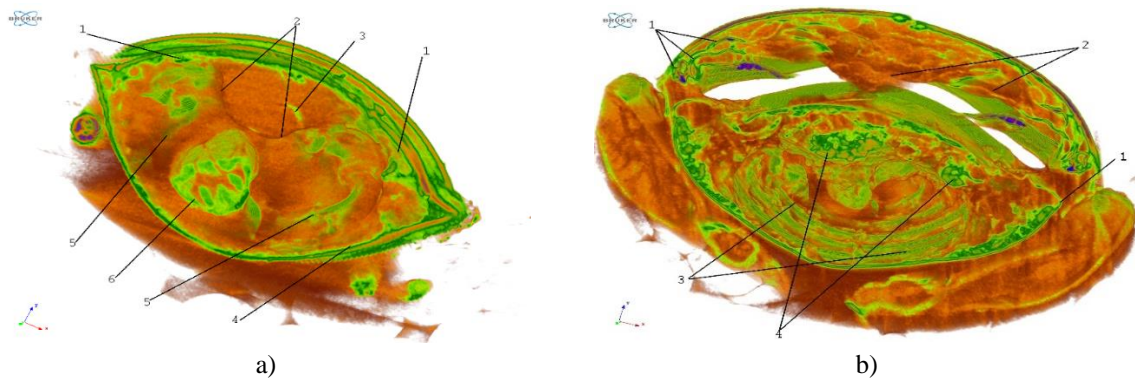


Figure 3. a) Anatomy of the back of the abdomen: 1- dorsal diaphragm; 2- perineural sinus; 3- ventral nerve cord; 4- ventral diaphragm; 5- pericardial sinus; 6- guts; b) Anatomy of the abdomen: 1- trachea; 2 - wing cavity; 3- ventral diaphragm; 4- fat body.

The midgut looks like a tube with short diverticula; in the cardiac section, they are somewhat longer and forward-pointing. The wall consists of single-layer epithelium. The midgut has a thin, single-layer peritrophic membrane along its entire length. The muscles of the midgut are well developed (**Figures 2b, 3b and 4a.2**). The hindgut is subdivided into the jejunum and rectum. Extending from the midgut/hindgut boundary are four malpighian tubules (**Figure 2a.8**). The malpighian tubules are straight and run in parallel with the hindgut almost to the apex of the abdomen (**Figure 2a**).

In insects, internal environment tissues include the hemolymph and the fat body. The circulatory system is well developed, the heart is large (**Figure 4**), and the hemolymph occupies most of the body cavity. Such developments can be explained by the large size of the beetle, which cannot rely on diffusion alone for substance transportation. Fat body cells fill most of the vacant body cavities (**Figures 2a and 3b**). These cells, which contain electronically transparent inclusions, come in a variety of shapes and range in sizes between 16 and 30 microns. The volume of the fat body strongly depends on the physiological state of the body, as is also the case with other insects, including the Silphidae [19]. The body cavity was shown to contain enocytes, cells that are found in many insects, the functions of which are not fully known [19].

The structure of the tracheal system shows robust development. Many well-branched tracheas are extending from the spiracles (**Figures 3b and 4a**) and reach all the organs and tissues, their longitudinal and transverse trunks being well visualized. Such developments have to do with the size of the body, which cannot sustain itself on oxygen diffusion alone. The tracheas, composed of the hypodermis and the intima, have a structure typical for insects [19]. The intima features spiral thickenings called tenidia.

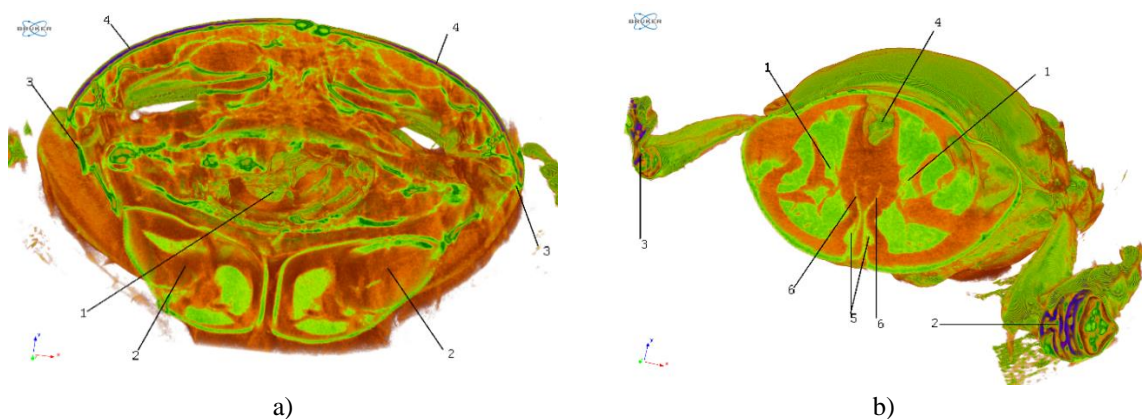


Figure 4. a) Anatomy of the abdomen: 1- a colon; 2-thigh muscles; 3- trachea; 4-chitin skeleton; b) Thoracic anatomy: 1- thoracic ganglion; 2- nerve endings of antennae; 3- nerve endings of the fore tarsus; 4- aorta; 5- frontal ganglion; 6- recurrent nerve.

The nervous system is divided into the central, peripheral, and sympathetic subsystems. The structure of the central nervous system (i.e. the brain) in *N. satanas* (**Figure 5**) shows a high level of complexity and compartmentalization [23]. The supra-pharyngeal ganglion features pronounced protocerebral, deutocerebral, and

tritocerebral regions; it hosts the associative centers and ganglion masses of the fused segments of the head (**Figure 5b**). The larger region, protocerebrum, has pronounced optical lobes (with three paired neuropilar structures and an ocellar center) (**Figure 5b**) that perceive and process sensory information coming from the complex eyes (**Figure 5a**). Notably, the cell bodies of the eye's sensory neurons are linked to the ocellar ganglia, from which ocellar nerves extend to the intercerebral part of the brain (**Figure 5**). The neuropilar subunits of the protocerebral bridge and the central body interconnect the symmetrical lobes of the protocerebrum. The mushroom bodies that adjoin the protocerebrum lobes on both sides are well visualized (**Figure 5b**). Their structure is complex: it shows Kenyon cells (KCs) with large neuroblasts (Nb) as well as pronounced associative links between the antennae (AGT) and the deeper layers (GC and Csh). The mushroom bodies of *N. satanas* are paired structures residing in the brain, each one being formed of 12 layers of neurons (Kenyon cells). Each mushroom body consists of four calyces (two on the right, two on the left) connected with the remaining parts of the brain via the so-called peduncles [23, 24].

The suprapharyngeal ganglion occupies most of the posterior half of the head; the subpharyngeal ganglion is shifted towards the prothorax and merges with the prothoracic ganglion. The mesothoracic ganglion is separated and well-developed (**Figure 5b**); the abdominal ganglia are linked with the metathoracic ones. The way the ganglia are organized is in line with the standard pattern [19, 24]. The bodies of the neurons are arranged perimetricaly, and the central part is occupied by the neuropil (**Figure 5b**). The body size of the neurons is 40–45 microns, while in other insects, their diameter ranges from 6 to 50 microns. There are, thus, approximately 107 neurons in the central nervous system, which number is significantly bigger than the average number of neurons found in insects (104–108) and fundamentally smaller than that observed in higher vertebrates (1025) [25]. The central nervous system occupies a relatively large portion of the body volume compared to that of other insects [26-29]. The structure of the peripheral nervous system generally matches the typical pattern observed in the Coleoptera order [24]. No elements of the sympathetic system have been identified, although they should be present [24]. The nerves of the antennae and the front legs (**Figure 4b**) are well-colored. The complex faceted eyes were highlighted in (**Figures 1 and 5**). For Kenyon cells, see (**Figure 5b**).

In *N. satanas*, like in most Coleoptera [19], the Endocrine system is represented by heterogeneous neurosecretory cells, a retrocerebral complex [19, 24], and neurohemal organs [23]. It is involved in controlling metabolic processes as it coordinates and integrates the activities of various body systems as well as complex behaviors [24]. At the same time, it is dominated by the nervous system and mediates its functions at the level of humoral influences. Coming out of the brain, the nerves travel to the cardiac bodies and adjacent cell bodies forming the retrocerebral complex (in *N. satanas*, this complex also consists of cardiac cell bodies which, besides the said connection to the 4 pairs of nerves extending from the brain, are also connected with the stomatogastric nervous system and, for the purposes hereof, are deemed to constitute its ganglia) [30].

Despite the large size of the beetle, the structure of the muscular system (**Figure 2b**) matches the typical pattern found in insects [24]. All the major muscle groups are present: the mouthpart muscles, the dorsal thoracic, and ventral longitudinal muscles; the dorsoventral muscles; the pleural muscles, the leg muscles, viz. dorsal abdominal, ventral longitudinal, and dorsoventral muscles (**Figure 2b**), and the muscles of the copulatory apparatus (**Figure 6b**). The main difference is in the number of myofibrils. The wing muscles are well developed and occupy a significant part of the thorax (**Figures 2b and 3b**).

The male reproductive system (in the specimen studied) (**Figures 2b and 6b**) consists of a pair of testes, a pair of vasa deferentia, an ejaculatory duct, accessory genital glands, and copulative apparatus. The copulative apparatus forms an external appendage called the genitals. The accessory glands open into the ejaculatory duct. The figure shows the right-hand testis and the respective accessory gland; the left-hand side seems to be out of sight due to poor contrast. Our dissection study has convincingly demonstrated that these organs are paired.

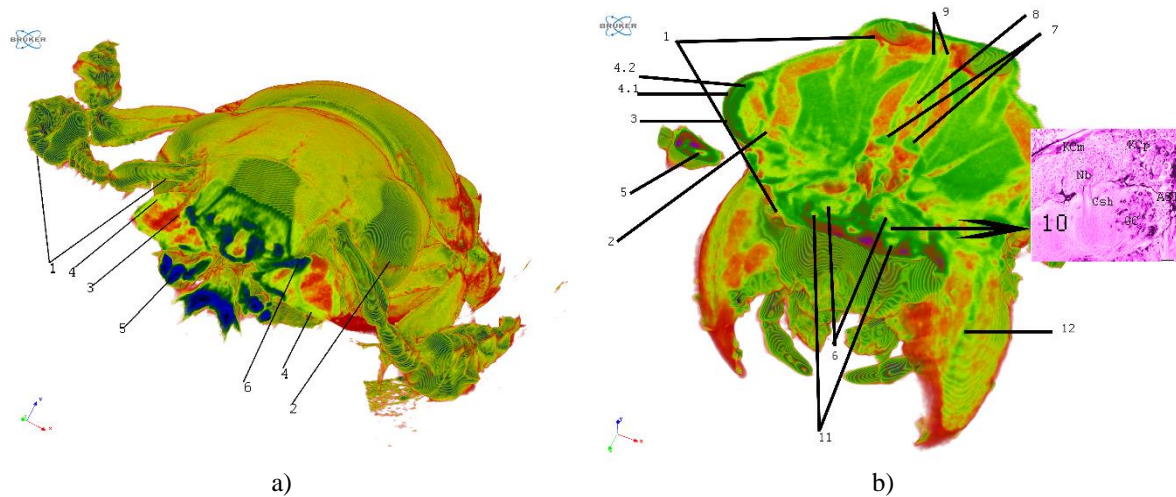


Figure 5. a) Head anatomy: 1- antenna; 2- compound eye; 3- salivary gland; 4- muscle; 5- nerve endings labium; 6- optic lobe; b) Head anatomy: 1- brain; 2- optic lobe; 3- cuticular lens; 41- nuclei of retinula cells; 42- retinula; 5- antenna nerve; 6- neurosecretory cells of brain; 7- neurosecretory cells of suboesophageal ganglion; 8- corpus allatum; 9- ventral nerve cord; 10- corpora pedunculata; 11- Kenyon cell; 12- mandibular nerves. №10 - the letter designations in the figure are: AGT - antenna-globular tract, Csh - rod fibers in the calyx, GC - glomeruli of the calyx, KCM - Kenyon medial cells, KCp - Kenyon peripheral cells, Nb - neuroblast [23].

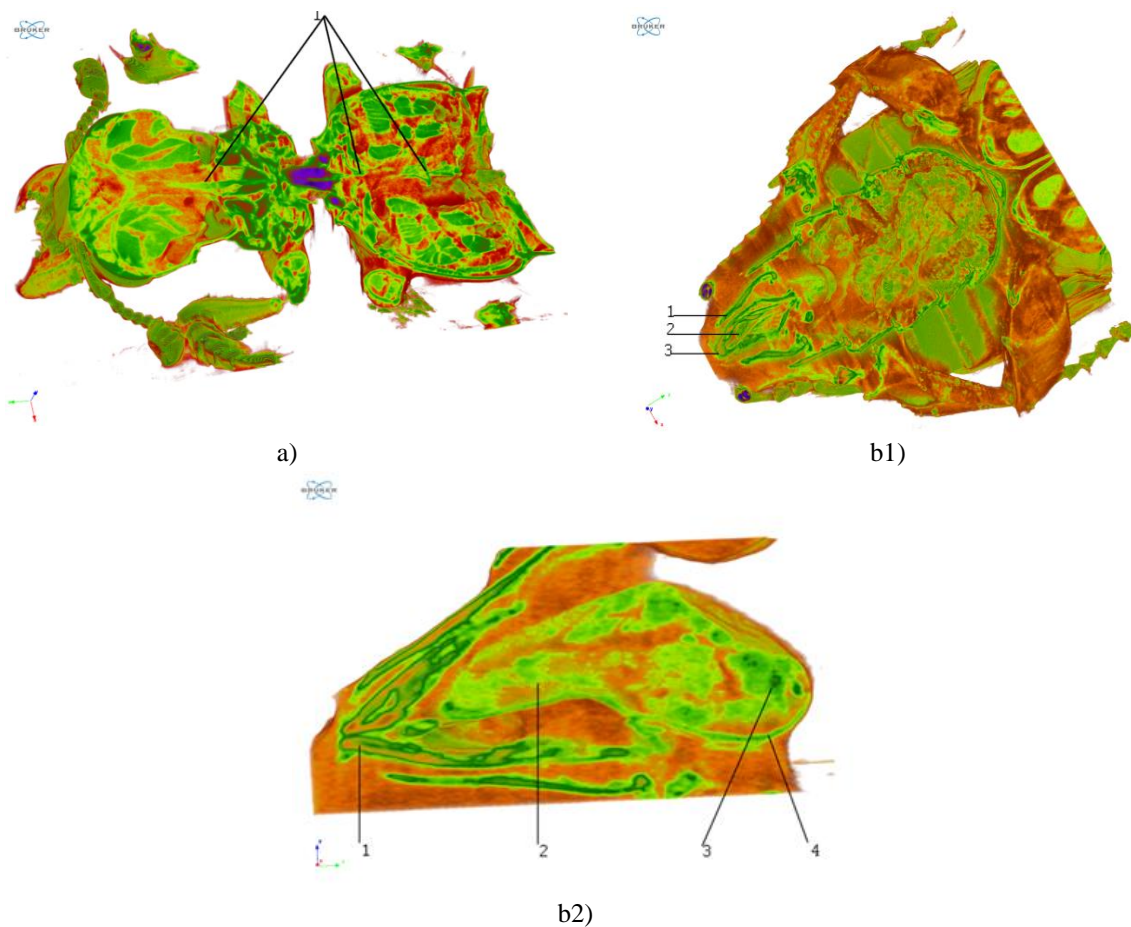


Figure 6. a) nerve cord: 1-nerve cord; b1) reproductive system (aedeagus): 1- penis parameres; 2- endophallus; 3- penis; b2) reproductive system: 1- aedeagus; 2- accessory genital glands; 3- male sex cells; 4- testis.

The results obtained show that the systems which undergo the biggest transformations are the metabolic systems (the digestive, circulatory, and tracheal systems) and the muscular system, which fact can be explained by the large body size. The biggest number of changes was observed in the nervous system [21].

As the size of the beetle increases, it becomes impossible for the capillary forces to efficiently maintain the circulation of hemolymph within the body, which is why *N. Satanus* has a well-developed heart, while hemolymph displaces the fat body. As the body size increases, so does the relative surface area of the intestinal epithelium, which, in the case, of *N. satanas*, is associated with the development of numerous short diverticula off the midgut wall. In addition to the absorption function, the diverticula may provide for the transport of nutrients, reducing the distance from the gut to the other organs.

The large body size contributes to the efficiency of active tracheal breathing. Because of this, *N. satanas*, with their 9 pairs of spiracles, have developed a relatively complex tracheal system. It is, thus, likely that the key transformations in the metabolic systems can be explained by the need to increase the efficiency of substance transportation within the body. The presence of qualitative changes in the nervous system attests to the complexity of its fundamental transformations associated with the quasi-social lifestyle [8, 15, 16].

As we see nutrition homogeneous (protein) food does not complicate the digestive system [19], this only led to the development of the intestinal tract.

Correlating the data obtained during the study of the brain *Nicrophorus* investigator [23], common features can be distinguished: the development of proto- and deutocerebrum and mushroom bodies pronounced cells Kenyon. The mechanisms underlying cognitive activity are being actively studied. It is proved that in the processes of associative learning, an important role is played by a heterogeneous population of glutamate receptors - the main excitatory mediator in the central nervous system of vertebrate and invertebrate animals. It is produced by neurosecretory brain cells. Causally related to touch processing information and the formation of associative memory.

CONCLUSION

We explain the larger size of the nervous system by the fact that the size of its neurons is significantly larger than that observed in most insects; in fact, their size is not far removed from the absolute maximum value corresponding to the size of the nucleus. The number of neurons in *N. satanas* is not large, but despite this, the relative volume of the central nervous system is much higher. This suggests the conclusion that an increase in the volume of the nervous system becomes possible when the beetles become big enough. At the same time, we observed fundamental differences in the structure of the central nervous system, which are associated with complex behaviors. The perception of odors and analysis thereof (smell of a carcass, a pheromone, an attractant), as well as the perception of sound signals (designed to attract the opposite sex or to warn of imminent danger), have contributed to the development of the central nervous system. The data obtained will help us to further monitor the development of the central nervous system in the *Nicrophorus* genus in the context of the evolution it went through when transitioning to the necrobiontic lifestyle.

As a result of microtomographic research, we found common features of the anatomical structure with small species of invertebrate animals primarily the digestive system, and the peripheral nervous system.

The quality of images obtained as a result of microtomography scanning depends on how the specimens were prepared. For best results, the specimens should be soaked in a contrasting solution (72 hours) and then dried before scanning. This produces a much greater difference in densities between the tissues being studied and the surrounding medium (in this case, air) compared to the scenario where the specimen is scanned in a liquid environment that is about as dense as its tissues. With this method, the resulting microtomographic cross-sections will boast higher contrast levels. We have prepared a VOI protocol which, in the future, will help accelerate similar research efforts focusing on other species of the genus.

ACKNOWLEDGMENTS : The authors are thankful to Dr. Igor Rzhepakovsky for assistance in carrying out microcomputing tomography.

CONFLICT OF INTEREST : None

FINANCIAL SUPPORT : None

ETHICS STATEMENT : The protocol for experiments with beetles complied with the requirements of the European Convention for the Protection of Vertebrate Animals used for Experimental and Other Scientific Purposes.

REFERENCES

1. Garcia FH, Fischer G, Liu C, Audisio TL, Economo EP. Next-generation morphological character discovery and evaluation: an X-ray micro-CT enhanced revision of the ant genus *Zasphinctus* Wheeler (Hymenoptera, Formicidae, Dorylinae) in the Afrotropics. *ZooKeys*. 2017;693:33-93. doi:10.3897/zookeys.693.13012
2. Poinapen D, Konopka JK, Umoh JU, Norley CJ, McNeil JN, Holdsworth DW. Micro-CT imaging of live insects using carbon dioxide gas-induced hypoxia as anesthetic with minimal impact on certain subsequent life history traits. *BMC Zool*. 2017;2(1):1-3. doi:10.1186/s40850-017-0018-x
3. Martín-Vega D, Simonsen TJ, Wicklein M, Hall MJ. Age estimation during the blow fly intra-puparial period: a qualitative and quantitative approach using micro-computed tomography. *Int J Legal Med*. 2017;131:1429-48. doi:10.1007/s00414-017-1598-2
4. Schmitt M, Uhl G. Functional morphology of the copulatory organs of a reed beetle and a shining leaf beetle (Coleoptera: Chrysomelidae: Donaciinae, Criocerinae) using X-ray micro-computed tomography. *ZooKeys*. 2015;547:193-203. doi:10.3897/zookeys.547.7134
5. Keklikoglou K, Faulwetter S, Chatzinikolaou E, Wils P, Brecko J, Kvaček J, et al. Micro-computed tomography for natural history specimens: a handbook of best practice protocols. *Eur J Taxon*. 2019;522:1-55. doi:10.5852/ejt.2019.522
6. Gignac PM, Kley NJ. Iodine-enhanced micro-CT imaging: Methodological refinements for the study of the soft-tissue anatomy of post-embryonic vertebrates. *J Exp Zool B Mol Dev Evol*. 2014;322(3):166-76. doi:10.1002/jez.b.22561
7. Pushkin SV, Nagdalian AA, Rzhepakovsky IV, Povetkin SN, Simonov AN, Svetlakova EV. AFM and CT study of zophoba smorio morphology and microstructure. *Entomol Appl Sci Lett*. 2018;5(3):35-40.
8. Pushkin SV. Carrion beetles (Coleoptera, Silphidae) of Russia. Atlas is the determinant Direct Media, Moscow. 2015:169. doi:10.13140/RG.2.1.1925.0325. (in Russian)
9. Smith DB, Bernhardt G, Raine NE, Abel RL, Sykes D, Ahmed F, et al. Exploring miniature insect brains using micro-CT scanning techniques. *Sci Rep*. 2016;6(1):1-0. doi:10.1038/srep21768
10. Fabre JH. The wonders of instinct. (Chap. 5, The burying beetles: experiments. Translated by B. Miall). London: T. Fisher Unwin Ltd. 1913, 320.
11. Steiger S, Stökl J. Pheromones regulating reproduction in subsocial beetles: insights with references to eusocial insects. *J Chem Ecol*. 2018;44:785-95. doi:10.1007/s10886-018-0982-9
12. Parapar J, Candás M, Cunha-Veira X, Moreira J. Exploring annelid anatomy using micro-computed tomography: A taxonomic approach. *Zool Anz*. 2017;270:19-42. doi:10.1016/j.jcz.2017.09.001
13. Reitter E. Uebersicht der mir bekannten schwarzen *Nicrophorus*-Arten. *Wien Entomol Ztg*. 1893;12:147.
14. Schedwill P, Geiler AM, Nehring V. Rapid adaptation in phoretic mite development time. *Sci Rep*. 2018;8(1):16460. doi:10.1038/s41598-018-34798-6
15. Pushkin SV. Extra-pair copulations in *nicrophorus humator* (Gleditsch, 1767)(*Nicrophorus* Kirby; Silphidae, Coleoptera). *Entomol Appl Sci Lett*. 2015;2(4):22-5.
16. Shippi AG, Paquet M, Smiseth PT. Sex differences in parental defence against conspecific intruders in the burying beetle *Nicrophorus vespilloides*. *Anim Behav*. 2018;136:21-9. doi:10.1016/j.anbehav.2017.12.011
17. Scott MP, Traniello JF. Behavioural and ecological correlates of male and female parental care and reproductive success in burying beetles (*Nicrophorus* spp.). *Anim Behav*. 1990;39(2):274-83. doi:10.1016/S0003-3472(05)80871-1
18. Haberer W, Schmitt T, Schreier P, Eggert AK, Müller JK. Volatiles emitted by calling males of burying beetles and *Ptomascopus morio* (Coleoptera: Silphidae: Nicrophorinae) are biogenetically related. *J Chem Ecol*. 2017;43:971-7. doi:10.1007/s10886-017-0892-2
19. Kumar N, Flammini F. YOLO-Based Light-Weight Deep Learning Models for Insect Detection System with Field Adaption. *Agriculture*. 2023;13(3):741. doi:10.3390/agriculture13030741
20. Kypke JL, Solodovnikov A. Every cloud has a silver lining: X-ray micro-CT reveals *Orsunius rove* beetle in Rovno amber from a specimen inaccessible to light microscopy. *Hist Biol*. 2020;32(7):940-50. doi:10.1080/08912963.2018.1558222

21. Kaan O. Micro-computed tomography (micro-CT) in medicine and engineering. Springer Nature Switzerland AG. 2020:312. doi:10.1007/978-3-030-16641-0
22. Nagdalian AA, Rzhepakovsky IV, Siddiqui SA, Piskov SI, Oboturova NP, Timchenko LD, et al. Analysis of the Content of Mechanically Separated Poultry Meat in Sausage Using Computing Microtomography. *J Food Compost Anal.* 2021;100:103918. doi:10.1016/j.jfca.2021.103918
23. Panov AA. Mushroom bodies in the brain of carrion beetles (Coleoptera, Silphidae). *Entomol Rev.* 2012;92:741-6. doi:10.1134/S0013873812070020
24. Raji JI, Potter CJ. The number of neurons in *Drosophila* and mosquito brains. *PLoS One.* 2021;16(5):e0250381. doi:10.1371/journal.pone.0250381
25. Makarova AA, Polilov AA. Structure of the Brain of the Smallest Coleoptera. In *Doklady Biochemistry and Biophysics* 2022 Aug (Vol. 505, No. 1, pp. 166-169). Moscow: Pleiades Publishing. doi:10.1134/S1607672922040068
26. Tiwari R, Singh I, Gupta M, Singh LP, Tiwari G. Formulation and Evaluation of Herbal Sunscreens: An Assessment Towards Skin Protection from Ultraviolet Radiation. *Pharmacophore.* 2022;13(3):41-9.
27. Rane BR, Gaikwad DS, Jain AS, Pingale PL, Gujarathi NA. Enhancement of pioglitazone hydrochloride solubility through liquisolid compact formulation using novel carrier neusilin Us2. *Pharmacophore.* 2022;13(3):64-71.
28. Yousefian M, Ghazi A, Amani F, Movaffagh B. Mortality rate in patients admitted to the ICU based on LODS, APACHE IV, TRIOS, SAPS II. *J Adv Pharm Educ Res.* 2022;12(1):56-62.
29. Taher SS, Al-Kinani KK, Hammoudi ZM, Mohammed Ghareeb M. Co-surfactant effect of polyethylene glycol 400 on microemulsion using BCS class II model drug. *J Adv Pharm Educ Res.* 2022;12(1):63-9.
30. Kavitha J, Sivakrishnan S, Srinivasan N. Self Medication in Today's Generation without Knowledge as Self Inflicted Harm. *Arch Pharm Pract.* 2022;13(3):16-22.